# Molecular Geometries of Acetylene and Ethylene Chemisorbed On Cu, Ni, Pd, and Pt Surfaces

Abstract: Ultraviolet photoemission measurements of the valence orbital electronic structure of acetylene and ethylene chemisorbed on Cu(100) or Cu(111), Ni(111), Pd(111), and Pt(111) are presented. We compare the measured energy levels of these chemisorbed species to those of the free molecule and use a similar comparison of the relative changes in ground state energy levels of distorted free molecules calculated with a SCF-LCAO (Self Consistent Field—Linear Combination of Atomic Orbitals) method to determine the molecular geometries of these chemisorbed species. The limitations and accuracies of such an approach are discussed. From the determined geometries we identify two trends in the structure of these chemisorbed molecules on these surfaces: first, increasingly greater molecular distortions occur with increasing atomic number of the substrate atom, and secondly, greater molecular distortions occur for ethylene than for acetylene on the same metal. These trends are consistent with a  $\pi$ -d bonding interaction and can be accounted for by the electronic structure of the substrate and of the molecule, respectively. With the exception of ethylene on Pd or Pt, we determine molecular geometries characteristic of small rehybridization. The molecular geometry of ethylene on Pd or Pt is generally characteristic of rehybridization to an sp<sup>3</sup> configuration.

### Introduction

The determination of the geometry of adsorbed hydrocarbon molecules on transition metal surfaces is an important problem which, for example, may provide a greater understanding of fundamental processes in heterogeneous catalysis. That is, the geometric structure not only reflects the nature and/or strength of the electronic interaction but may also influence surface reactions. The surface structure problem can be further divided into two related aspects: the location of the molecule relative to the surface atoms and the geometry of the adsorbed molecule itself. This latter, molecular geometry reflects the state of hybridization of the carbon atoms in the hydrocarbon molecule and is important in understanding the chemistry of the adsorbed molecule.

Several approaches have been taken to obtain structural information about chemisorbed hydrocarbon species. Low energy electron diffraction (LEED) intensity analysis has proved to be a powerful technique for determining the locations of atoms on surfaces [1-4]. In particular such an analysis for a phase of acetylene adsorbed on Pt(111) has been used to determine the locations of the carbon atoms in these species relative to the Pt(111) substrate atoms [5]. Although this determination of bond site rules out several previously postulated bonding models, more detailed information about the adsorbed species cannot be obtained since present LEED analyses lack the

sensitivity to distinguish CC bond distances to within  $\pm$  0.01 nm (0.1 Å) or to determine H atom locations [5]. Such limitations would appear to restrict the use of LEED as a method to obtain structural information relevant to the chemistry of adsorbed hydrocarbon or other organic molecules on surfaces.

Another approach in determining molecular geometries is to perform theoretical calculations of the total energy for all possible geometries of the adsorbed molecule on a transition metal surface so as to determine the geometry that provides the lowest total energy state of the system. Such an approach is not based upon an analysis of experimental observables and depends upon accurate, detailed theoretical models of fairly complex systems. To date no rigorous *ab initio* calculations have been performed for hydrocarbon molecules on any surface. However, a semi-empirical theoretical model has been used by Anderson [6] to determine the geometries of acetylene and ethylene on a cluster of Ni atoms which simulate the Ni(111) surface.

In this work we discuss and apply a method by which the molecular geometries of chemisorbed acetylene and ethylene can be obtained from their electronic structure as measured experimentally by means of ultraviolet (UV) photoelectron spectroscopy. The ability to use the electronic structure to obtain geometric information results

Copyright 1978 by International Business Machines Corporation. Copying is permitted without payment of royalty provided that (1) each reproduction is done without alteration and (2) the *Journal* reference and IBM copyright notice are included on the first page. The title and abstract may be used without further permission in computer-based and other information-service systems. Permission to *republish* other excerpts should be obtained from the Editor.

from the strong interdependence of geometric and electronic structure. A similar approach has been used to obtain insight into the structure of amorphous semiconductors [7], the structure of silicon surfaces [8, 9], and the structure of hydrogen surface compounds on Si [10], where other conventional structural methods, such as x-ray diffraction or LEED intensity analyses, are either inapplicable or not yet tractable for these systems.

Here, we use the measured energy levels of the  $\sigma$ -orbital valence bonds of acetylene and ethylene chemisorbed on Cu, Ni, Pd, and Pt single-crystal surfaces, together with the corresponding eigenvalues for distorted molecules obtained from molecular orbital calculations, to determine the molecular geometries of these particular chemisorbed species. We present evidence that such use of ground state eigenvalues and distorted free molecule calculations (simplifications needed to render structural analysis tractable) may not introduce significant errors. Finally, we note that this work represents an extension of an earlier photoemission study of hydrocarbons on a Ni(111) surface, where we used molecular orbital calculations to place a limit on the degree of rehybridization occurring for acetylene, ethylene, propylene and benzene chemisorbed on Ni(111) [11]. Previous UV photoemission studies of adsorbed hydrocarbons have generally used ionization levels as a "fingerprint" to characterize the chemical nature of the adsorbed hydrocarbon [12–15].

### **Experimental procedure**

The present studies were performed in a turbomolecularpumped UHV system whose base pressure is less than  $1.3 \times 10^{-8}$  Pa (1 ×  $10^{-10}$  torr). For UV photoemission the system is equipped with a rare gas dc resonance lamp which produces unpolarized radiation, and an angle-integrating double pass cylindrical mirror electron energy analyzer (CMA). The system also contains facilities for low energy electron diffraction studies, a UTI quadrupole mass spectrometer for thermal desorption studies, and an auxiliary electron gun for Auger electron spectroscopy. Single-crystal samples of Cu(111), Ni(111), Pd(111), and Pt(111) were prepared by conventional techniques [16] and mounted on a multiple sample holder which permitted the samples to be cooled with liquid nitrogen to  $T \approx$ 80 K or resistively heated to  $T \approx 1600$  K as measured with a Chromel-Alumel thermocouple spot-welded to the back of the crystal. The Cu(111) sample was damaged in the course of this study and was replaced with a Cu(100) crystal. The Cu(100) crystal was prepared in an auxiliary system by vapor epitaxial growth on a chemically polished MgO(100) substrate held at  $T \approx 750$  K. (Polycrystalline Cu films were also formed in situ by the evaporation of Cu onto a polycrystalline Ta substrate and were also examined.) The single-crystal samples were cleaned by mild oxidation treatments, argon ion sputter-etching, and subsequent annealing [16]. Surface characterization was performed by LEED, Auger, and photoemission analyses. Research grade purity Matheson ethylene (99.98%) and purified Matheson acetylene (>99.6%) were used and examined for other impurities by mass spectroscopy. In particular, the acetylene extraction procedures used to load our gas manifold provided essentially acetone-free acetylene. The ratio of mass 43 to mass 26, the principal mass numbers for acetone and acetylene, respectively, was 1/750 for ionizer voltages that produce 70-V electrons and 15-V ions. The pressures and exposures cited here are based on uncorrected ion gauge readings. The actual pressure at the sample may have been slightly lower since the sample was located in another part of the system inside a magnetic shield for the CMA.

Energy analysis of the photoemitted electrons was performed with the CMA operated in a fixed pass mode so as to have a minimum resolution of  $\approx 0.15$  eV for He I ( $h\nu =$ 21.2 eV), and  $\approx 0.25$  eV for He II ( $h\nu = 40.8$  eV) work. These two photon energies provide wider energy windows than Ne I ( $h\nu = 16.8 \text{ eV}$ ) or Ne II ( $h\nu = 26.9 \text{ eV}$ ) radiation and, therefore, were used almost exclusively. Operation of the windowless resonance lamp introduces some rare gas into the chamber which contributes to an increase in the system pressure. The total pressure increase we observe is  $< 1.3 \times 10^{-8} \, \text{Pa} \, (1 \times 10^{-10} \, \text{torr})$  and it consists primarily of the rare gas. The samples could be rotated with their normal direction in the plane defined by the axis of the CMA and the photon beam. The photon beam lies 73° off the axis of the CMA, and we nominally chose the sample normal to be 20° from the axis of the CMA into the photon beam, so as to collect electrons over a wide range of emission angles. We believe our results to be characteristic of angle-integrated spectra, since changes in the sample orientation did not change the observed adsorbate-derived ionization energies. In some instances changes in the sample orientation did modify the relative intensities of ionization features. Work functions and their changes were measured by using the lowenergy cutoffs of the photoemission energy distributions.

### **Experimental results**

In order to emphasize the electronic levels of the adsorbed species as well as to facilitate a direct comparison of these levels on the different substrates, we choose to display "difference" spectra. The "difference" spectra, or  $\Delta N(E)$  spectra, are obtained by taking the photoemission spectra N(E) of the surface having adsorbed species and subtracting the N(E) spectra of the clean surface. Thus, such  $\Delta N(E)$  spectra reflect both the emission from occupied valence orbitals of chemisorbed acetylene as well as the attenuation of substrate emission associated with the presence of the overlayer and any alterations in the electronic structure of the surface atoms of the sub-

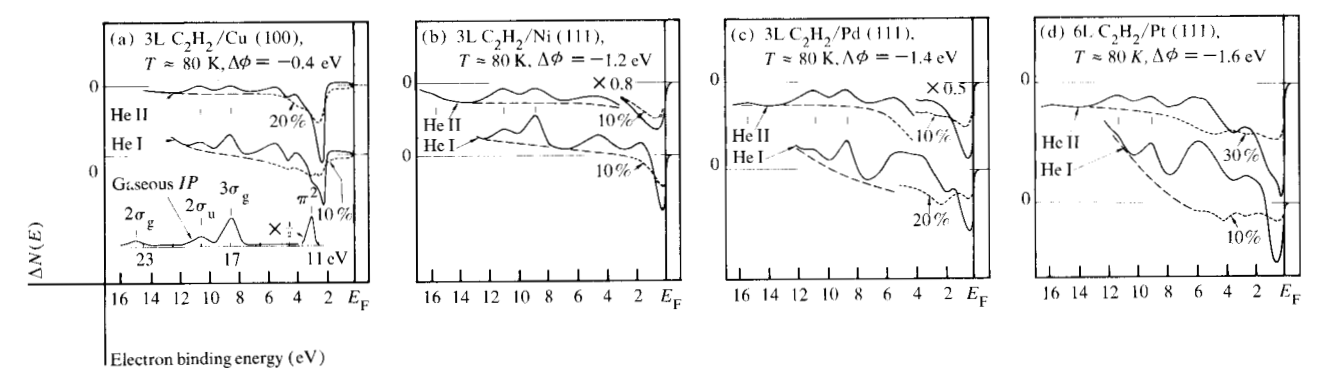


Figure 1 Difference in emission  $\Delta N(E)$  from clean surfaces of (a) Cu(100), (b) Ni(111), (c) Pd(111), and (d) Pt(111) for both  $h\nu = 21.2$  eV (He I) and  $h\nu = 40.8$  eV (He II) after saturation exposures of  $4 \times 10^{-4}$  Pa-s (3 langmuirs) to acetylene or  $8 \times 10^{-4}$  Pa-s (6 langmuirs) for Pt(111), all with the samples held at  $T \approx 80$  K. Indicated in each panel is the corresponding work function change as well as a uniform attenuation of the d bands (short dashed lines) and estimated change in background emission (long dashed lines). All electron binding energies are referred to the Fermi level. In panel (a) for comparison we show the ionization levels ( $h\nu = 40.8$  eV) of gaseous acetylene, which were obtained with a spectrometer of similar resolution and geometry [18]. The small vertical lines indicate the central position of each ionization feature, i.e. the vertical ionization levels, to which we compare.

strate. For convenience we reference the electron binding energies of our photoemission measurements to the Fermi level  $E_{\rm F}$ . In order to show the location of the d bands and any preferential d-band attenuation for each surface in Fig. 1, we use the short dashed lines to indicate the effect of a uniform d-band attenuation both for  $h\nu=21.2$  and 40.8 eV. The estimated change in secondary electron background is indicated by the longer dashed line.

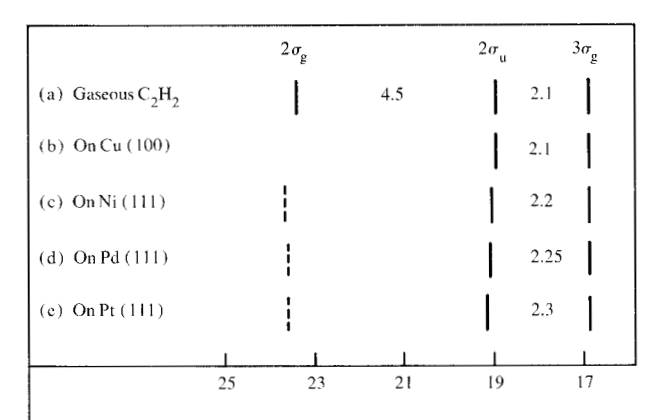
The spectra shown in Fig. 1 are each representative of saturation coverage of a single phase of acetylene that forms on the clean surface at  $T \approx 80$  K, before we observe any coverage-dependent changes characteristic of the onset of formation of a second layer of "physically" adsorbed acetylene. Here we are interested in this initial phase of chemisorbed acetylene on each surface, and we find their corresponding  $\Delta N(E)$  spectra to be similar. In spite of these similarities, we note striking differences upon warming the samples. At higher temperatures on Cu(100) this phase of acetylene reversibly desorbs, while on Ni(111) this phase is stable until  $T \approx 400$  K where it starts to decompose to carbon and hydrogen. In contrast, this initial phase of acetylene on Pd(111) or Pt(111) converts for T > 200 K or 300 K, respectively, to form an "olefinic" C,H, species that starts to decompose to carbon and hydrogen at  $T \approx 460 \text{ K}$  [17].

The relative locations and intensities of the ionization features for this initial phase of chemisorbed acetylene that lie further than  $\approx 8$  eV below  $E_{\rm F}$  on each metal are similar to those occurring for gas phase acetylene. In Fig. 1(a) we show the ionization spectra for gas phase acetylene taken in a spectrometer of geometry and energy resolution similar to that used for our studies [18]. We can readily relate the  $2\sigma_{\rm g}$ ,  $2\sigma_{\rm u}$  and  $3\sigma_{\rm g}$  molecular orbitals of

gas phase acetylene to the ionization features we observe for chemisorbed acetylene. We derive average relaxation/screening shifts [19] of 4.1, 3.5, 3.7, and 3.5 eV, respectively, from the  $2\sigma_{n}$ - and  $3\sigma_{e}$ -derived ionization features.

The additional ionization features for acetylene chemisorbed between  $\approx 3-7$  eV can be related to the  $1\pi^2$  orbitals of gaseous acetylene. As discussed previously for initially chemisorbed acetylene on Ni, Pd, and Pt, the  $1\pi^2$ orbitals are shifted closer to the  $\sigma$  orbitals relative to the gas phase by  $\approx 1.2, 1.9, \text{ and } 2 \text{ eV}, \text{ respectively } [17]. Such$ a shift is indicative of  $\pi$ -d bonding [12, 20]. For acetylene on Cu(100) two well-resolved ionization features at 4 and 5 eV below  $E_{\rm F}$  are observed in the  $\Delta N(E)$  spectra for both  $h\nu = 21.2$  and 40.8 eV. These two features could be attributed to the  $1\pi^2$  orbitals shifted 1.2 and 2.6 eV, i.e., a lifting of the degeneracy of the  $1\pi^2$  orbitals by the surface. We also observe these same two features for acetylene on polycrystalline Cu, as was found by Yu et al. [14]. Although we find some suggestion of a splitting of the  $1\pi^2$ derived levels for acetylene on Pd(111) or Pt(111), the strong redistribution of d states at the bottom of the dband characteristic of the  $\pi$ -d interaction [21] causes uncertainties in relating such features to only the  $\pi$  orbitals of chemisorbed acetylene. We find no indication of a  $1\pi^2$ orbital splitting for acetylene on Ni(111) aside from the breadth of the  $\pi$  levels.

In this work our interest lies in the relative positions of the higher-lying  $\sigma$  levels, since these levels reflect the chemical nature of the molecule. In Fig. 2 we summarize the relative  $\sigma$ -orbital-derived vertical ionization potentials (*IP*) of gaseous acetylene and the corresponding ionization levels of chemisorbed acetylene as deduced from our results at both photon energies. We note that the location of the  $2\sigma_v$ -derived ionization features indicated by



Relative vertical IP (eV)

Figure 2 Summary of the  $\sigma$ -orbital-derived vertical ionization potentials (*IP*) of gaseous acetylene [18, 24] relative to the corresponding ionization levels of chemisorbed acetylene, which are shown in Fig. 1. The  $3\sigma_g$ -derived levels are aligned and we denote the separation in eV between pairs of levels. The locations of the  $2\sigma_g$ -derived levels for acetylene on Ni, Pd and Pt are less certain and are indicated as such by the short dashed lines (see text).

the dashed lines in Fig. 2 is more uncertain than that of the other levels due to its low intensity and overlap with the onset of d-band emission from  $h\nu=23.7$  eV radiation. Here, chemisorption-induced d-band attenuation of the 23.7-eV signal may have cut off the larger binding energy side of this peak so as to make it appear at slightly smaller binding energies. Although it is clear that acetylene on these surfaces is chemically similar in each case to gaseous acetylene, we find a trend in the widening of the separation between the  $2\sigma_{\rm g}$ - and  $3\sigma_{\rm g}$ -derived ionization levels in going from Cu to Pt, which we shall consider in detail later.

In Fig. 3 we show  $\Delta N(E)$  spectra at  $h\nu = 21.2$  and 40.8 eV for ethylene chemisorbed at  $T \approx 80$  K onto clean Cu(111), Ni(111), Pd(111) and Pt(111) surfaces. As before, these spectra represent saturation coverages of an initial phase of chemisorbed ethylene which forms before multilayer adsorption. We note that spectra for ethylene chemisorbed on either Cu(100) or Cu(111) at  $T \approx 80 \text{ K}$ have the same relative ionization levels. For comparison we also show in Fig. 3(a) the ionization features for gas phase ethylene again obtained in a spectrometer of similar geometry and resolution to that used in our studies. Comparison to these levels indicates that the 1b<sub>au</sub> orbital, the  $\pi$  orbital, appears to be shifted toward the 1b<sub>2g</sub> ionization level relative to the gas phase levels, indicative of  $\pi$ -d bonding [12, 21]. We note that the exposure of ethylene to Ni or Pd at higher temperatures (T > 200 K) [or warming to T > 200 K] results in the chemical reaction of ethvlene with the surface to form chemisorbed hydrogen and an acetylenic or "olefinic"  $C_2H_2$  species, respectively, which we have discussed elsewhere [12, 17]. These species appear to be identical in UPS to the phase formed directly from acetylene. However, we find that ethylene on Pt converts to a new "olefinic" phase which contains more hydrogen, i.e., more  $\sigma_{\rm CH}$  orbitals, than the  $C_2H_2$  "olefinic" phase which forms from acetylene on Pt. Ethylene on Cu(111) reversibly desorbs upon warming.

We summarize in Fig. 4 the  $\sigma$ -orbital-derived vertical IP of gaseous ethylene and the corresponding ionization levels of chemisorbed ethylene, again determined from both  $h\nu=21.2$  and 40.8 eV results. Here, we show that the relative  $\sigma$ -derived ionization levels for chemisorbed ethylene are more strongly modified from those in the gas phase than is the case for acetylene. The average relaxation/screening shifts [19] for ethylene on these surfaces are approximately 1.9, 2.3, 2.0, and 2.9 eV, respectively, as determined from the  $1b3_u$ -,  $3a_g$ -, and  $1b_{2g}$ -derived orbital ionization features.

## Structure of initially chemisorbed acetylene and ethylene

The similarities in the relative ionization levels of initially chemisorbed and gas phase acetylene or ethylene indicate that the surface species are chemically similar to their gas phase counterparts. The differences that exist in these ionization energies relative to those in the gas phase contain geometric information about the chemisorbed molecule. Fortunately, we find two approximations that simplify an analysis of these differences so as to make a structural analysis tractable without introducing significant errors. First we use calculations of distorted free molecules for all reasonable combinations of CC and CH bond distances and HCC and HCH bond angles to assess how geometric changes from the equilibrium gas phase geometry affect orbital energies. We then correlate the differences in ionization levels we observe experimentally between gaseous and chemisorbed molecules to the differences in energy levels found theoretically, to derive the geometry of the chemisorbed hydrocarbon.

A simple physical basis exists for the use of a free molecule approximation and  $\sigma$ -orbital energies to obtain structural information regarding chemisorbed unsaturated hydrocarbons. Namely, the electrons in the hydrocarbon  $\sigma$ -valence orbitals are shielded by the  $\pi$  electrons and separated in both space and energy from the substrate d electrons so as to reduce any direct  $\sigma$ -d interaction. For molecular chemisorption the  $\pi$ - and  $\sigma$ -valence electrons are largely coupled as they are in the free molecule. Here any distortions in the  $\pi$ -electron charge density caused by  $\pi$ -d bonding influence the geometry of the molecule, which in turns alters the  $\sigma$ -electron charge density and the eigenvalues via the intramolecular interaction. The preservation of molecular character implies that the  $\sigma$  eigenvalues

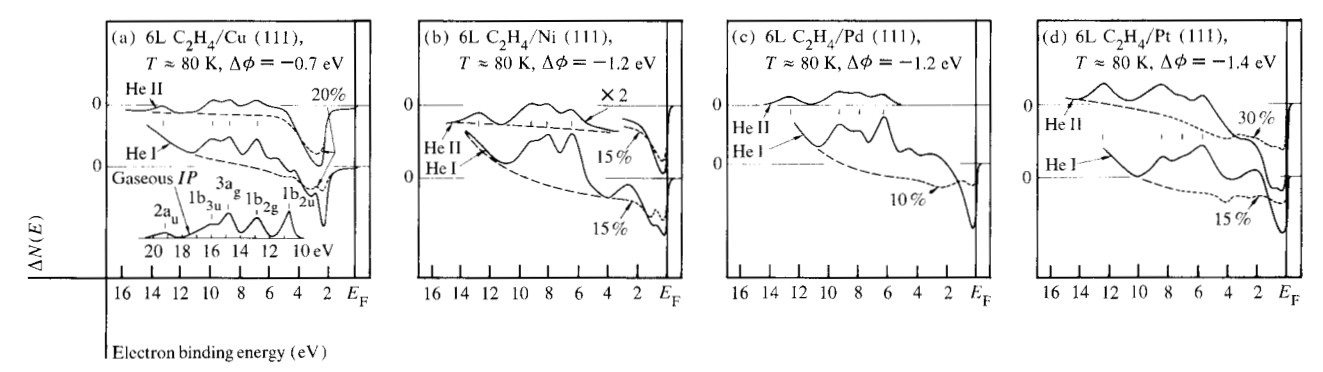
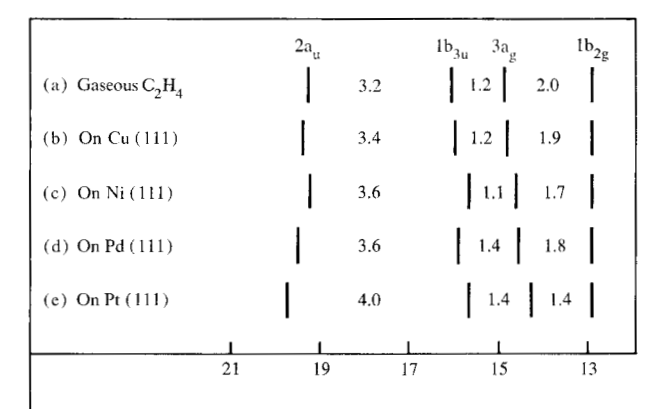


Figure 3 Difference in emission from clean surfaces of (a) Cu(111), (b) Ni(111), (c) Pd(111), and (d) Pt(111) for  $h\nu = 21.2$  eV (He I) or  $h\nu = 40.8$  eV (He II) after saturation exposure of  $8 \times 10^{-4}$  Pa-s (6 langmuirs) to ethylene with the samples held at  $T \approx 80$  K. Indicated in each panel is the corresponding work function change as well as a uniform attenuation of the d bands (short dashed lines) and estimated change in background emission (long dashed lines). All electron binding energies are referred to the Fermi level. In panel (a) for comparison we show the ionization level of gaseous ethylene ( $h\nu = 21.2$  eV) which was obtained with a spectrometer of similar resolution and geometry [18]. Here we have labeled the molecular orbitals of ethylene according to a coordinate system where the molecule lies in the x, z plane. The small vertical lines indicate the central positions of each ionization feature, i.e., the vertical ionization levels, to which we compare.

still characterize the geometry in the same manner as in the free molecule. Finally, the possible shielding of the  $\sigma$  electrons by the  $\pi$  electrons, as well as the similar localization of electrons in each of the higher-lying  $\sigma$ -valence orbitals relative to the surface, would lead to similar initial-state screening and final-state relaxation effects for these  $\sigma$ -valence orbitals. To the extent that these conditions are valid, the observed differences in relative  $\sigma$ -orbital ionization energies between these chemisorbed molecules and their gas phase counterparts directly reflect changes in the molecular geometry that have occurred upon chemisorption.

More quantitative results indicate the validity of the aforementioned qualitative arguments. First, free molecule calculations are supported by recent SCF X- $\alpha$  multiple-scattering calculations of ethylene interacting with one atom of Ni, Pd or Pt [21] or two atoms of Ni [20], extended Hückel calculations of gaseous and distorted acetylene on Ni clusters [6, 22], and our own SCF-LCAO calculations of gaseous and distorted acetylene and ethylene on Be clusters. These calculations indicate that the presence of the metal atom or atoms alone does not significantly affect the relative ground state energies of the higher-lying  $\sigma$ -valence orbitals. Further, the detailed changes in the orbital energies of the high-lying  $\sigma$  levels that occur upon distortion of the molecule appear to be independent of whether metal atoms are present. Empirical evidence also suggests that σ-orbital-dependent changes in final-state screening and relaxation effects associated with the presence of the surface are not significant for these chemisorbed species. That is, we find that the valence orbital ionization levels for monolayer coverages of a variety of adsorbed saturated hydrocarbon

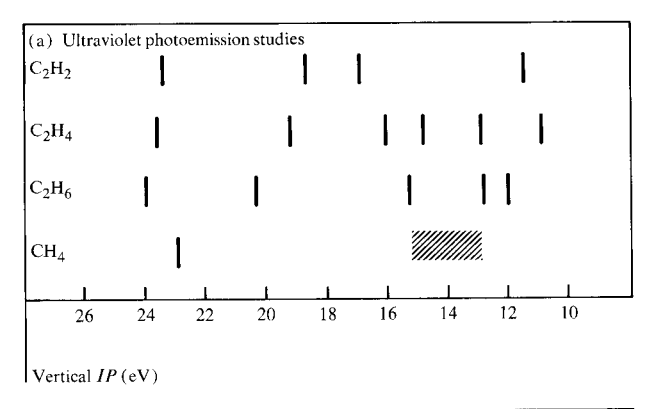


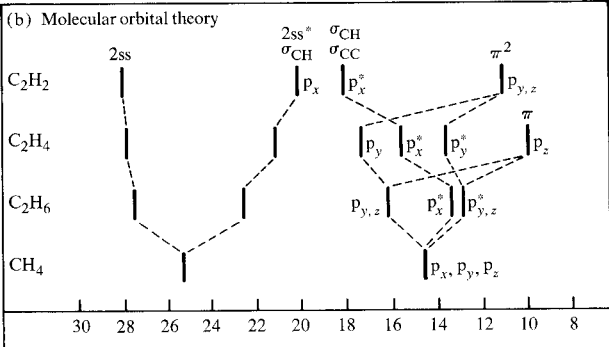
Relative vertical IP (eV)

Figure 4 Summary of the  $\sigma$ -orbital-derived vertical ionization potentials (*IP*) of gaseous ethylene [18, 24] relative to the corresponding ionization levels of chemisorbed ethylene, which are shown in Fig. 2. Here we have labeled the molecular orbitals of ethylene according to a coordinate system where the molecule lies in the x, z plane. The  $1b_{2g}$ -derived levels are aligned and we denote the separation in eV between pairs of levels.

molecules on Ni [11] or on Cu, Pd and Pt surfaces, as well as for condensed unsaturated or saturated hydrocarbons on these surfaces, are uniformly shifted from those of their gas phase counterparts. Possible errors introduced by these approximations will be discussed later.

For our free molecule calculations we use GAUSSIAN-70, an *ab initio* SCF-LCAO molecular orbital calculation [23], with a 4-31G basis set. These calculations require core storage of about 250 kilobytes and computation times of about 12 or 28 seconds per geometry for acetylene or ethylene, respectively, on an IBM 370/168 com-

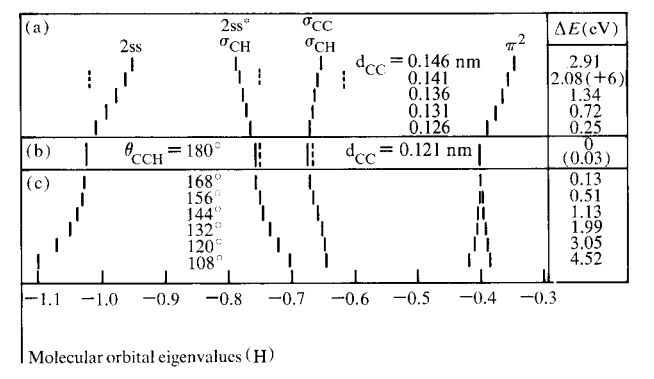




Molecular orbital eigenvalues (eV) (GAUSSIAN -70, 4-31 G basis)

Figure 5 Comparison of gas phase vertical ionization potentials (top) [18, 24-26] to our calculated ground state energy levels (bottom) for gas phase acetylene, ethylene, ethane, and methane. The ionization band from  $\approx 13-15$  eV for methane is associated with Jan-Teller distortions of the ion [26]. These ground state levels were calculated using an *ab initio* SCF-LCAO Hartree-Fock method [23] with a 4-31G basis. The principal C(2p) atomic components of the high-lying valence molecular orbitals are shown where the x direction lies along the CC bond direction. The principal bonding character(s) of the various molecular orbitals for acetylene is indicated.

Figure 6 The geometric dependence of the eigenvalues of acetylene calculated using an *ab initio* SCF-LCAO Hartree-Fock method [23]. The equilibrium geometry is shown in panel (b) while panels (a) and (b) show the effect of either CC bond expansion or CCH bond angle reduction, respectively. The change in Hartree-Fock energy upon distortion from the gas phase geometry is represented by  $\Delta E$ . The dashed lines in panel (b) are for a CH bond distance of 0.110 nm while those in panel (a) are for a CCH bond angle of 132° and a CC bond distance of 0.141 nm. The principal orbital character of the  $3\sigma_{\rm g}$ ,  $2\sigma_{\rm u}$ , and  $2\sigma_{\rm g}$  molecular levels is indicated. The hartree energy unit (H) equals 27.2 eV.

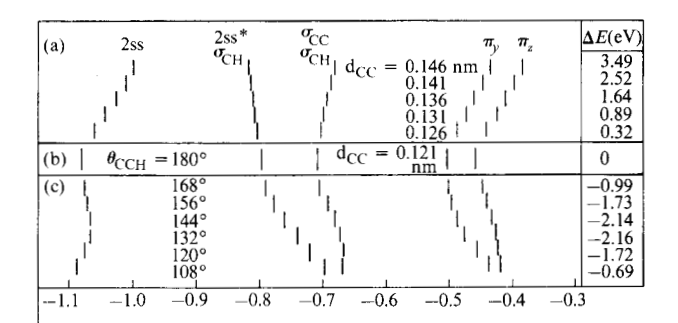


puter. In order to demonstrate that the relative ground state energy level positions of these molecular orbital calculations can be accurately related to vertical ionization potentials (*IP*) we show a comparison of our calculated eigenvalues and *IP* for acetylene [18, 24], ethylene [18, 24], ethane [18, 25, 26], and methane [25, 26] in Fig. 5. Here we have chosen the energy scales to allow visual comparison of *relative* level positions. Although some differences in the trends are noted [for example, in the relative locations of the low-lying C(2ss) levels], we observe rather good agreement between measured ionization levels and the relative ground state energy levels we calculate for free molecules. We expect these calculations to predict the relative changes in ionization levels for distorted free molecules with similar accuracy.

In our previous work to investigate possible rehybridization effects of unsaturated hydrocarbons on Ni [11], we performed similar calculations on distorted molecules for specific geometries expected to be characteristic of a particular degree of rehybridization. Here we make no such assumptions and take combinations of many possible geometric distortions. For acetylene we have performed these calculations for all combinations of CC bond distances from 0.121 to 0.146 nm in 0.005-nm increments with CCH bond angles from 180° to 108° in 12° increments. This represents 42 geometries, each with a fixed CH bond length of 0.106 nm. We have also examined CH bond lengths for acetylene of 0.108 nm and 0.110 nm for several selected geometries to establish how CH bond length variations affect the eigenvalues. Similarly for ethylene we have calculated all combinations of geometries for CC bond lengths from 0.134 to 0.154 nm in 0.005-nm increments, CCH bond angles from 120.0° to 106.85° in 2.63° increments, and HCH bond angles from 120° to 104.30° in 2.63° increments, each with a fixed CH bond distance of 0.110 nm. This represents 245 geometries. Here the CH bond distance of 0.110 nm was initially selected since this CH bond length is found in Zeise's salt [27], but we have also examined other CH bond lengths of 0.107 and 0.108 nm to again determine how variations in CH bond length affect the eigenvalues. Finally, we note that from the dependence of these eigenvalues upon changes in CH or CC bond distances or CCH or HCH bond angles we could reliably extrapolate calculated eigenvalues to the next increment of each geometric parameter from the actual geometries considered. This represents a possible total of 216 geometries for acetylene and 1134 geometries for ethylene. Geometric distortions involving a rotation of the CH or CH, groups about the CC bond axis of acetylene or ethylene, respectively, were also considered but were not found to be of consequence in the present analysis and are not discussed here.

In Fig. 6 we illustrate how geometric distortions typically modify the eigenvalues of acetylene either for a change in CC bond distance [Fig. 6(a)] or for a change in CCH bond angle from the equilibrium gas phase geometry of acetylene [Fig. 6(c)]. Here we label the eigenvalues according to their principal bonding character(s). We also indicate by the dashed lines in Fig. 6(b) the eigenvalues for acetylene with a CH bond distance of 0.110 nm. For all geometries we indicate the change in Hartree-Fock energy  $\Delta E$  from the equilibrium gas phase acetylene geometry. Although the shifts in eigenvalues depend upon the particular changes in geometry, similar trends exist, for example, in how variations in CCH bond angles change eigenvalues for other CC bond distances. Thus, for a CC bond distance of 0.141 nm, a change in the CCH bond angle from 180° to 132° shifts the 2ss  $(2\sigma_{o})$  eigenvalue downward and the 2ss\*  $(2\sigma_u)$  and  $\sigma_{cc}$   $(3\sigma_g)$  eigenvalues upward as indicated by the dashed levels in Fig. 6(a). We also find that for some combinations of CC bond lengths and CCH bond angles the relative separation between  $2ss (2\sigma_{\alpha})$  and  $2ss^* (2\sigma_{\alpha})$  eigenvalues can remain unchanged. A similar effect is also observed for the  $2ss* (2\sigma_{ij})$  and  $\sigma_{cc} (3\sigma_{g})$  levels, where the increased separation occurring for an increased CC bond length can be offset in some cases by a decrease in the CCH bond angle. Thus, the use of only two of these three  $\sigma$ -orbital eigenvalues for geometry determination (for example, the  $2\sigma_{ij}$ and  $3\sigma_{\mu}$  levels) can lead to non-unique geometries.

In order to demonstrate that the bonding of acetylene to other atoms does not strongly alter the geometric dependence of the  $\sigma$ -orbital eigenvalues shown in Fig. 6 for free acetylene, we display in Fig. 7 similar SCF-LCAO calculations for acetylene bonded to a Be atom. Here the Be atom lies at a distance of 0.1943 nm from each of the carbon atoms, and we only show the eigenvalues for the acetylene-derived molecular orbitals. From our calculations we find that bonding arises from an interaction of the Be(2s) states with the  $\pi_{ij}$  orbitals of acetylene. Although the absolute eigenvalues differ in Figs. 6 and 7 for the same molecular geometry, the geometric dependence or changes in  $\sigma$ -level separations from those of the undistorted molecule for both free and "bonded" acetylene are nearly identical. The differences in these geometric dependencies give rise to small 0.035-eV RMS deviations (or 0.001-eV, excluding  $\theta_{\rm HCH} \lesssim 120^{\circ}$ ) in the relative  $\sigma$ -level separations of the free and "bonded" molecule. An important point to note in comparing Figs. 6 and 7 is that even though the Be-acetylene interaction leads to an energetically preferred new geometry having  $\theta_{\rm HCH} \approx 135^{\circ}$ , the  $\sigma$ -level spacings obtained in the free molecule calculation characterize this geometry as well as in the complete calculation. We find similar results for other Be-C distances and other bonding sites on up to four Be atoms. Thus, the  $\sigma$ -level eigenvalues obtained in distorted free molecule calculations provide an accurate description of the dependence of the  $\sigma$ -level spacings for acetylene

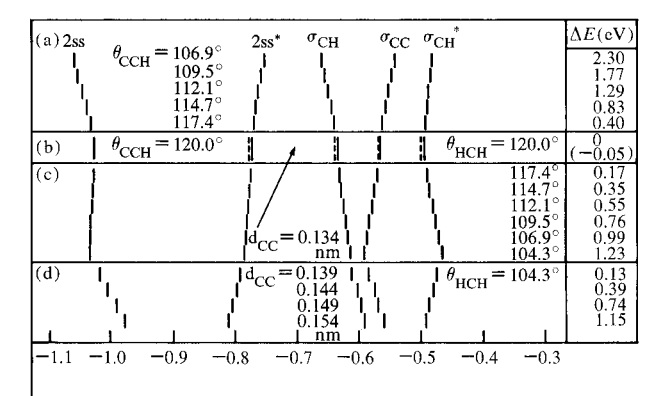


Molecular orbital eigenvalues (H)

Figure 7 The geometric dependence of the acetylene-derived eigenvalues for acetylene bonded to a Be atom calculated using an ab initio SCF-LCAO Hartree-Fock method [23]. The Be atom lies in the plane of the molecule at a distance of 0.1943 nm from each carbon atom. The molecular geometry of acetylene is identical to that used in Fig. 6, where panel (b) shows the eigenvalues for the gaseous molecule, panel (a) for CC bond expansions, and panel (c) for CCH bond-angle reductions. The change in Hartree-Fock energy upon distortion from the equilibrium gas phase geometry is represented by  $\Delta E$ . As observed from  $\Delta E$ ,  $\theta_{\rm CCH} \approx 135^{\circ}$ provides a lower total energy and is a preferred bonding geometry over a linear geometry. The principal orbital characters of the  $3\sigma_e$ ,  $2\sigma_u$  and  $2\sigma_e$  molecular levels are indicated. We note that the  $\pi_{\mu}$  molecular level is shifted to smaller energies due to both bonding with the Be(2s) states (not shown) as well as the admixture of the C(2s) atomic orbital into the  $\pi_u$  orbital, i.e., a rehybridization of the  $\pi_y$  orbital to facilitate bonding. The hartree energy unit (H) equals 27.2 eV.

bonded to Be. As mentioned earlier, other results [6, 20–22] suggest a similar situation for acetylene and ethylene bonded to transition metal atoms. Hence, free molecule calculations would appear to provide a useful, time-saving approximation for obtaining geometric information from the energy levels of chemisorbed molecules.

The geometric dependences of the valence orbital eigenvalues of ethylene are shown in Fig. 8 for a fixed CH bond distance of 0.110 nm. We again label these eigenvalues according to their principal bonding character. In Fig. 8(b) the eigenvalues for the gas phase geometry of ethylene, i.e., a CH bond distance of 0.108 nm, are shown by the dotted lines. Again we find that changes in the CH bond length for other geometries tend to shift the eigenvalues in the same manner. Both the larger number of  $\sigma$  levels observed for ethylene than for acetylene and the manner by which these  $\sigma$  levels change upon geometric distortion enables us to determine a unique ethylene geometry from the experimentally observed levels. For example, although an increase in the CH bond distance tends to produce a relative shift in the  $\sigma_{cc}$  (3a<sub>g</sub>) level characteristic of an increased HCH bond angle, it also produces a shift in the 2ss\* (2a, ) level relative to the  $\sigma_{\rm CH}$  (1b<sub>30</sub> and 1b<sub>2g</sub>) levels that is not characteristic of an increased HCH bond angle.



Molecular orbital eigenvalues (H)

**Figure 8** The geometric dependence of the eigenvalues of ethylene calculated using an *ab initio* SCF-LCAO Hartree-Fock method [23]. The eigenvalues for gas phase ethylene are shown in panel (b) for CH bond distances of 0.110 nm (solid lines) and 0.107 nm (dashed lines). The effects of CCH bond angle reduction, HCH bond angle reduction and CC bond expansion are shown in panels (a), (c), and (d), respectively. The change in Hartree-Fock energy  $\Delta E$  from the gas phase geometry having a CH bond distance of 0.110 nm is indicated for each distortion. The principal orbital character of the  $1b_{2g}$ ,  $3a_g$ ,  $1b_{3u}$ ,  $2a_u$ , and  $2a_g$  molecular levels is indicated. The hartree energy unit (H) equals 27.2 eV.

**Table 1** Molecular structures of acetylene on Cu(100), Ni(111), Pd(111) and Pt(111) surfaces at  $T \approx 80$  K as prescribed by bond distances d and bond angles  $\theta$ . Also shown is  $d_{\perp}$ , the distance from the plane containing the hydrogen atoms to the CC bond axis, and  $\Delta E$ , the change in Hartree-Fock energy for this distorted geometry. The CH bond distance cannot be determined (see text). An ambiguity exists in determining the CC bond lengths and CCH bond angles directly and we indicate a "preferred" structure by  $(\dagger)$  as discussed in the text. The overall accuracies are discussed in the text.

	$d_{\rm CC}$ (nm)	$ heta_{ m CCH}$	$d^{\perp}$ (nm)	$\Delta E (eV)$
/Cu(100)	†0.121	180–169°	0-0.022	0.065
	0.126	114°	0.098	3.871
/Ni(111)	†0.123	180-168°	0-0.022	0.188
	0.126	117°	0.095	3.273
/Pd(111)	†0.123	168°	0.022	0.251
	0.126	120°	0.093	3.15
	0.131	114°	0.098	10.60
/Pt(111)	†0.126	168°	0.022	0.374
	†0.123	144°	0.063	1.23
	0.126	126°	0.086	2.73
	0.131	117°	0.095	10.51

In order to compare these calculated levels to the ionization levels that we observe experimentally we cannot directly compare absolute energies or differences; these are uncertain because of limitations and approximation in the calculation such as the treatment of exchange-correlation, basis set effects, etc., as well as the fact that we do not calculate ionization energies. In view of the apparent

uniformity of final-state screening and relaxation effects for adsorbed hydrocarbons as mentioned earlier, and the close correspondence between gas phase eigenvalues and IP of gaseous molecules shown in Fig. 5, we believe that a scaling of the changes in relative energy level separations between gaseous and chemisorbed phases should be a reasonable procedure for comparing experiment to our calculations. Thus, for a given chemisorption system we take the calculated  $\sigma$ -level separations for the free molecule and change these level separations in proportion to the corresponding change in  $\sigma$ -level separations observed between the corresponding gaseous and chemisorbed phase ionization levels. We thereby determine a new set of energy levels, which have been scaled so as to allow comparison with the calculated eigenvalues. From this comparison we determine the geometry that best reproduces these experimentally derived levels.

The molecular geometries determined in this manner for acetylene and ethylene on Cu, Ni, Pd, and Pt are shown in Tables 1 and 2, respectively. Indicated in each table is  $d_{\perp}$ , the separation between the plane containing the hydrogen atoms and the CC bond axis, as well as  $\Delta E$ , the change in Hartree-Fock energy for each molecular geometry from the equilibrium gas phase geometry. In Table 2 we also indicate for comparison the molecular structure of ethylene in Zeise's salt as determined by a recent neutron diffraction study [27]. (Zeise's salt is an organometallic compound that contains an ethylene molecule bonded to a single Pt atom and thereby provides an interesting comparison to ethylene chemisorbed on Pt.)

For acetylene the uncertainty in the location of the  $2\sigma_{\mu}$ level introduces a complication into determining structures. That is, if we neglect the  $2\sigma_g$  level due to the uncertainties in its location, we cannot determine unique geometries. In this case we find a (continuous) range of acetylene geometries which match the observed  $2\sigma_{u}$ - $3\sigma_{\sigma}$ level separations. The structures with larger CC bond distances and with smaller CCH bond angles arise from compensating effects in the geometric dependencies of these eigenvalues as described earlier. Thus, we indicate in Table 1 some of the combinations of the CC bond distances and CCH bond angles which describe the observed  $2\sigma_{\rm u}$ - and  $3\sigma_{\rm g}$ -level separations. However, the large change in energies calculated for some of these geometries, such as that on Cu and Ni or Pd and Pt with CC bond lengths of 0.126 or 0.131 nm (or greater), respectively, would suggest these as unlikely geometries. The remaining geometries then occur over a narrow range of CC bond distances. Further, based upon the approximate separation between the observed  $2\sigma_{ij}$  and  $2\sigma_{g}$  levels (within  $\approx 0.3$  eV of that observed in the gas phase), we could rule out acetylene structures with CCH bond angles smaller than 130°. Thus, although we cannot unambiguously determine geometries, our present results support certain geometries

**Table 2** Molecular structure of ethylene on Cu(111), Ni(111), Pd(111) and Pt(111) surfaces at  $T \approx 80$  K as prescribed by bond distances d and bond angles  $\theta$ . Also shown is  $d_1$ , the distance from the plane containing the hydrogen atoms to the CC bond axis and  $\Delta E$ , the change in Hartree-Fock energy for this distorted geometry. The overall accuracies are discussed in the text. ( $d_{\perp}$  for ethane = 0.052 nm).

	$d_{\mathrm{CC}}$ (nm)	d <sub>CH</sub> (nm)	$ heta_{ ext{HCH}}$	$\theta_{\mathrm{CCH}}$	$d_{\perp}$ (nm)	$\Delta E$ (eV)
/Cu(111)	0.134-0.139	0.107	120°	120-117.4°	0.012	0.133
/Ni(111)	0.139	0.110	117.4°	120°	0.016	0.347
/Pd(111)	0.144	0.110	106.8-109.5°	106.8-109.5°	0.054	2.71
/Pt(111)	0.149	0.110	106.8°	106.8–109.5°	0.056	2.96
Zeise's Salt [27]	0.1375	0.110	114.9°	121.0°	0.016	

which we indicate in Table 1 and which we refer to as "preferred" geometries. Work is currently in progress using filtered He II radiation to determine the precise location of the  $2\sigma_u$  level and pin down the geometry of acetylene on these surfaces.

To determine the overall accuracies of our analysis we must consider several sources of uncertainties. These are derived from the sensitivity of the calculated eigenvalues to molecular distortions, the  $\pm 0.05$ -eV uncertainties in the relative ionization levels we observe [28], and the errors introduced by the approximations within our analysis. We can estimate the errors introduced in the scaling procedures used for relating the changes observed in IP to our calculated eigenvalues by considering how differences in the scaling procedure, i.e., scaling different combinations of pairs of orbitals, affect the determined geometry. Such errors arise since the relative eigenvalues do not identically reproduce the IP (Fig. 5) for gaseous molecules. We find that as a result of the sensitivity of the calculated eigenvalues to geometric distortions and the already close correspondence between IP and eigenvalues, the determined geometry is almost independent of the scaling procedure. Namely, of the nine ways to scale ethylene IP, we find all give rise to the same molecular structure on Cu or Ni, while on Pd and Pt one scaling procedure gives rise to a different structure that differs from the others by a CCH or HCH bond angle of 2.63°. Thus, uncertainties produced by our procedure of comparison to ground state eigenvalues would appear to be small.

The neglect of transition metal atoms in our calculations and the occurrence of non-geometry-derived level shifts introduce small errors that can also be estimated. For example, screening of the molecule by the electrons of the substrate atoms may reduce the antibonding character of a  $C(2ss^*)$  molecular orbital so as to shift it to lower energies relative to the other levels. In one calculation [21] such a shift is found to be substrate atom dependent, being the largest ( $\approx 0.05 \text{ eV}$ ) for Pt. Although we

do not observe any noticeable change in separation between the corresponding  $C(2ss^*)$ –C(2ss) levels for monolayer adsorption of ethane on Pt relative to gaseous ethane, the lack of consideration of such a 0.05-eV shift in the  $C(2ss)^*$  level of, for example, ethylene would primarily result in an overestimation of the CC bond expansion by  $\approx 0.0025$  nm. Similar screening effects would be expected also for the  $2\sigma_n$  orbital of acetylene.

Bearing in mind such procedural uncertainties, we estimate that the overall accuracy of our analysis is about  $\pm 0.0025$  nm for CC bond lengths,  $\pm 2.63^{\circ}$  or  $\pm 6^{\circ}$  for HCC bond angles for ethylene or acetylene, respectively,  $\pm 2.63^{\circ}$  for HCH bond angles and  $\pm 0.002$  nm for CH bond distances for ethylene. For distortions characteristic of strong rehybridization of the carbon atoms in the adsorbed molecule, we expect these limits of accuracy to become larger due to the eventual breakdown of the approximations used.

Another potentially important source of uncertainties in our analysis arises from possible nonuniformities in final-state relaxation effects [11-13]. Although empirical evidence suggests these to be small, as mentioned earlier, such shifts may be larger for chemisorbed species than those found for physisorbed saturated hydrocarbons or condensed unsaturated hydrocarbons. One theoretical calculation of CO bonded "end-on" to one and two Ni atoms recently found that although the relaxation shifts of the high-lying valence levels are dependent on the number of Ni atoms used, they are uniform to within ≈0.1 eV for the case of two Ni atoms—the case likely to best simulate the final-state effects produced by a surface [29]. Although the degree of uniformity of final-state relaxation effects for the high-lying valence orbitals of chemisorbed hydrocarbons is still largely unknown, we expect these nonuniformities to be smaller than in the case of CO on Ni. This is expected as a result of the likely geometry of the chemisorbed hydrocarbon on the surface, i.e., lying flat on the surface, and as a result of the similar spatial

orientation on the surface of the high-lying  $\sigma$ -valence orbitals of the unsaturated hydrocarbons. We also anticipate that to first order, any nonuniform relaxation effects will shift the measured levels on each surface in a similar fashion, thereby allowing us to achieve accurate relative structures. Clearly, if such nonuniform level shifts can be theoretically estimated or determined, they can be applied as a correction to the measured level positions so as to enable more accurate structure determinations.

### Discussion of molecular geometries

First, we can compare our detailed structural results for acetylene and ethylene on Ni(111) to the modified extended Hückel results of Anderson [6, 22] where the geometries of these molecules on small Ni clusters were selected on the basis of total energy optimization. Anderson's results indicate CC bond expansions of ≈0.02 nm and a decrease in the CCH bond angle by 45-55° from those of the free molecules. These are geometry changes substantially greater than those found in our analysis. The energy levels for Anderson's determined geometries indicate energy level shifts from the undistorted molecule which are characteristic of those we find in our free molecule calculations when similar distortions occur. However, the small changes in ionization levels experimentally observed between gaseous or chemisorbed acetylene or ethylene on Ni are not consistent with Anderson's predicted geometries. Such a discrepancy could arise from nonuniform relaxation shift, but likely does not, since an unreasonable 1-eV differential level shift in the  $2\sigma_{\rm u}$  and  $3\sigma_{\rm g}$  levels would be necessary to reconcile these differences. Thus, we believe that the large molecular distortions predicted by Anderson may have resulted, for example, from his choice of parameters [30], from the use of small clusters that neglect adsorbate-adsorbate interactions, or from the lack of self-consistency in his calculations which may permit excessive charge transfer [31]. We do not compare our structural results for the low-temperature phase of chemisorbed acetylene on Pt(111) to the structure of a room-temperature phase of acetylene on Pt(111), deduced in a LEED intensity analysis by Kesmodel et al. [5], since these phases are not equivalent [17].

Since no other structural results exist for hydrocarbon molecules on surfaces, we now discuss the qualitative trends in the geometries of acetylene and ethylene on the different transition metal surfaces. The relative trends in these geometries are expected to be quite reliable regardless of the simplifications of our analysis. Further, we do not expect our consideration of acetylene on Cu(100) rather than on Cu(111) to affect such trends, since little if any crystallographic dependencies were found for ethylene on Cu(100) and Cu(111). In summary, we find stronger distortions in the molecular geometries for the heavier substrate atoms, i.e., increasing distortions in go-

ing from Cu or Ni to Pt. Also, the CC bond distortions for ethylene appear to be generally larger and correspond to a proportionally greater degree of rehybridization than for our "preferred" structure of acetylene on these surfaces. We find that both these trends can be qualitatively accounted for on the basis of the electronic structure of these surfaces and molecules as well as the occurrence of a  $\pi$ -d bonding interaction.

A  $\pi$ -d bonding interaction is commonly believed to occur for unsaturated hydrocarbons in organometallic transition metal compounds. Here bonding involves the admixture of occupied metallic d states with unoccupied molecular  $\pi^*$  states and occupied molecular  $\pi$  states with occupied metallic d\* states, so as to produce both dative and retrodative ("backbonding") bonding components, respectively [32]. The backbonding component not only provides the main contribution to the heat of adsorption [12], i.e., bonding energy, but is also thought to be responsible for the distortions within the bonded molecule [33]. Here we expect a stronger  $\pi$ -d bonding interaction to occur with the Pd and Pt substrate atoms, since their d wavefunctions are more spatially extended and can more readily overlap with  $\pi$  and  $\pi^*$  molecular orbitals [21]. Thus, the stronger distortions we observe for ethylene or acetylene on Pd and Pt surfaces vs the Cu or Ni surface can be attributed to the greater  $d \rightarrow \pi^*$  backbonding component of a stronger  $\pi$ -d bonding interaction. This increased  $\pi$ -d interaction is also reflected in the increased  $\pi$ -orbital bonding shift for acetylene on these surfaces, as previously discussed [17]. A similar increase in the  $\pi$ -orbital bonding shift for ethylene as a function of substrate likely occurs on these surfaces as well, but it is difficult to accurately separate ionization features of the  $1b_{21}(\pi)$  orbital from the  $1b_{2g}(\sigma)$  orbital.

In addition, we can associate a stronger CC bond distortion of chemisorbed ethylene relative to that of chemisorbed acetylene with the electronic structure of these molecules. In general the  $\pi$ - $\pi$ \*-level separation should be larger in acetylene than in ethylene since the carbon atoms are located closer together in acetylene than in ethylene. This is found to be true for the triplet  $\pi \to \pi^*$  excitation of gas phase ethylene and acetylene where the transition energies are found to be 4.4 eV [34] and 5.3 eV [35], respectively. Using the locations of the unperturbed  $\pi$  levels for acetylene and ethylene on these surfaces, 3-4 eV vs 3.5-4.5 eV below  $E_{\rm F}$ , respectively, as well as the  $\pi \to \pi^*$  excitation energies for acetylene and ethylene, we can position the unperturbed  $\pi$  and  $\pi^*$  levels of acetylene and ethylene relative to the substrate d states. The unperturbed  $\pi^*$  level for acetylene would then lie above the unperturbed  $\pi^*$  level for ethylene,  $\approx 1\frac{1}{2}$  eV further from the occupied d bands. Thus, even though we expect an upward shift of both  $\pi^*$  levels associated with the  $\pi^*$ -d interaction, the smaller separation between the initial  $\pi^*$ 

level and the highest-lying occupied d states for ethylene than for acetylene would permit a stronger  $\pi$ -d backbonding interaction for ethylene. As before, this stronger backbonding interaction for chemisorbed ethylene can lead to greater molecular distortions than that for chemisorbed acetylene.

Another noteworthy distinction between the structures of acetylene and ethylene on these surfaces is the relatively strong distortion of ethylene on Pd and Pt. That is, while the CC bond distortions for acetylene are relatively small and appear to vary uniformly from one surface to the next, the distortions for ethylene on Pd and Pt are markedly greater than on Cu or Ni or in Zeise's salt. In particular, our analysis for ethylene on Pd and Pt shows that the hydrogen atoms are strongly bent away from the CC bond axis, even more than for pure sp<sup>3</sup> hybridization of the carbon atoms. However, while the hydrogen atom locations are characteristic of sp<sup>3</sup> hybridization, neither our determined CC bond distances nor the 3.6-4.0-eV splitting between the 2ss\* and higher-lying  $\sigma$ -level-derived ionization features are characteristic of complete sp<sup>3</sup> hybridization. The lack of an sp<sup>3</sup>-hybridized CC bond distance for ethylene on Pd and Pt may arise by necessity for optimal spatial overlap of d and  $\pi$  wavefunctions; i.e., an olefinic CC bond distance may be better matched to the Pd or Pt substrate. Perhaps this strongly distorted phase of ethylene on Pd and Pt may be related to the olefinic phase of acetylene on Pd and Pt that occurs for  $T \ge$ 200 K [17] and 300 K, respectively. Clearly, we cannot answer such questions at present and again caution that our geometric results become less certain for these large distortions. However, the larger distortions for ethylene chemisorbed on Pt than for ethylene in Zeise's salt are consistent with the formation of bonds to several Pt atoms, which is not possible in the salt.

Finally, the relative ionization intensities for ethylene on Pd and Pt also show an interesting difference from those observed for free ethylene or ethylene on Cu or Ni. This difference may be related to the location of the hydrogen atoms in ethylene on Pd and Pt. Namely, we find that the  $\sigma_{\rm CH^-}$  (1 $b_{\rm 3u^-}$  and 1 $b_{\rm 2g^-}$ ) derived ionization features of chemisorbed ethylene on Pd or Pt are more intense relative to the  $\sigma_{\rm CC}$ - (3a<sub>g</sub>-) derived ionization feature than on Ni or Cu (see Fig. 3). This relative enhancement of CH orbitals on Pd and Pt may reflect stronger emission due to a bending of these orbitals well out of the plane of the surface, and our preferential collection of this emission by our electron energy analyzer. Alternately, stronger rehybridization for ethylene on Pd or Pt may tend to mix the  $\pi$ -derived states into the  $\sigma_{\rm CH}$  orbitals as occurs for ethane [see Fig. 5(b)]. Angle-resolved and polarizationdependent photoemission studies such as those recently performed for CO on Ni [36, 37] and Pt [37] will probably provide further insight into such questions.

### **Conclusions**

We have determined the molecular geometries of acetylene and ethylene chemisorbed on Cu, Ni, Pd, and Pt surfaces at  $T \approx 80$  K by means of comparisons of the relative ionization levels of gaseous and chemisorbed species to eigenvalues obtained from SCF-LCAO calculations of distorted free molecules. Despite the several approximations which are used to render the present structural analysis tractable, we argue that structural determinations can be made and that, in particular, the structural trends will be reliable.

We conclude that at  $T \approx 80$  K acetylene adsorbs on all surfaces as a  $\pi$ -bonded species which is not strongly rehybridized. Although uncertainties in the position of a low-lying level for chemisorbed acetylene place more uncertainty in our structural determination for acetylene, we find a clear trend toward increasing geometric distortions as the atomic number of the substrate atoms increases. This trend can be related to an enhanced  $\pi$ -d backbonding interaction associated with the greater spatial extent of the d wavefunction of the heavier transition metal atoms. For chemisorbed ethylene at  $T \approx 80 \text{ K}$  we not only observe a similar dependence of the molecular geometry on the substrate but also greater CC bond distortions than for our "preferred" structure of acetylene. We can relate these greater distortions to a stronger  $\pi$ -d "backbonding" interaction which may arise due to an expected smaller transition energy between occupied d states of the metal and  $\pi^*$  states of ethylene than for acetvlene. Although the geometries of chemisorbed ethylene on Cu and Ni at  $T \approx 80$  K are characteristic of a weakly distorted, nearly planar molecule, ethylene on Pd and Pt at these same temperatures appears to be generally distorted into an sp<sup>3</sup> hybridization configuration.

### Acknowledgment

The author wishes to acknowledge useful conversations with A. B. Anderson and R. P. Messmer regarding unpublished work as to how molecular orbital eigenvalues of distorted molecules are affected by the presence of transition metal atoms. This work was partially supported by the Office of Naval Research.

### References and notes

- J. A. Strozier, Jr., D. W. Jepsen, and F. Jona, Surface Physics of Materials, Vol. 1, J. M. Blakely, ed., Academic Press, Inc., New York, 1975, pp. 1-77.
- J. B. Pendry, Low Energy Electron Diffraction Theory, Academic Press, Inc., London, 1974.
- S. Y. Tong, Progress in Surface Science, Vol. 7, part 2, S.
   G. Davison, ed., Pergamon Press, Inc., Oxford, 1975.
- 4. J. E. Demuth, J. Colloid Interface Sci. 58, 184 (1977).
- L. L. Kesmodel, P. C. Stair, R. C. Baetzold, and G. A. Somorjai, *Phys. Rev. Lett.* 36, 1316 (1976).
- Alfred B. Anderson, J. Chem. Phys. 65, 1729 (1976); 62, 1187 (1975).
- 7. J. D. Joannopoulos and M. L. Cohen, *Phys. Rev. B* **8**, 2733 (1973).

- 8. J. A. Appelbaum and D. R. Hamann, *Phys. Rev. Lett.* 31, 106 (1973); 34, 806 (1974).
- K. C. Pandey and J. C. Phillips, Phys. Rev. Lett. 34, 1450 (1975).
- K. C. Pandey, T. Sakurai, and H. D. Hagstrum, *Phys. Rev. Lett.* 35, 1728 (1975).
- 11. J. E. Demuth and D. E. Eastman, *Phys. Rev. B* 13, 1523 (1976).
- J. E. Demuth and D. E. Eastman, *Phys. Rev. Lett.* 32, 1123 (1974); D. E. Eastman and J. E. Demuth, *Jpn. J. Appl. Phys. Suppl.* 2, 827 (1974).
- 13. E. W. Plummer, B. J. Waclawski, and T. V. Vorburger, Chem. Phys. Lett. 28, 510 (1974).
- K. Y. Yu, W. E. Spicer, I. Lindau, P. Pianetta, and S. F. Lin, Surface Sci. 57, 157 (1976).
- G. Broden and T. N. Rhodin, Chem. Phys. Lett. 40, 247 (1976).
- 16. J. E. Demuth and T. N. Rhodin, Surface Sci. 42, 261 (1974).
- 17. J. E. Demuth, Chem. Phys. Lett. 41, 12 (1977).
- 18. W. D. Grobman, private communication.
- 19. We define the average screening/relaxation shift  $\Delta E^{\rm SR}$  as

$$\Delta E^{\rm SR} = \sum_{i=1}^{N} \frac{(\mathit{IP} - \mathit{BE})_i}{N} - (\phi_{\rm clean} + \Delta \phi_{\rm sat}),$$

where IP is the gas phase ionization potential, BE the binding energy relative to  $E_{\rm F}$  for the corresponding level, and  $\phi_{\rm clean}$  +  $\Delta\phi_{\rm sat}$  represents the saturation coverage work function. The average of the difference between IP and BE is taken over the N valence orbitals observed. (We note that for physisorbed or condensed hydrocarbons IP - BE appears to be the same for each valence orbital.)

- 20. N. Rösch and T. N. Rhodin, *Phys. Rev. Lett.* 32, 1189 (1974); private communications.
- R. P. Messmer, The Physical Basis for Heterogeneous Catalysis, E. Drauglis and R. I. Jaffee, eds., Plenum Press, New York, 1975, p. 261.
- 22. A. B. Anderson, to be published.
- R. Ditchfield, W. J. Hehre, and J. A. Pople, *J. Chem. Phys.* 54, 724 (1971).
- D. G. Streets and A. W. Potts, J. Chem. Soc. Faraday Trans. II 70, 1505 (1974).

- A. W. Potts and D. G. Streets, J. Chem. Soc. Faraday Trans. II 70, 875 (1974).
- J. N. Murrell and W. Schmidt, J. Chem. Soc. Faraday Trans. II 68, 1709 (1972).
- Richard A. Love, T. F. Koetzle, G. J. B. Williams, L. C. Andrews, and R. Bau, *Inorg. Chem.* 14, 2653 (1975).
- 28. The uncertainties in relative ionization levels here are less than in previous studies [12-15] due to our use of two photon energies and our ability to compare experimentally similar gas phase results.
- P. S. Bagus and K. Hermann, Solid State Commun. 20, 5 (1976); K. Hermann and P. S. Bagus, Phys. Rev. B 15, 3661 (1977).
- R. P. Messmer, C. W. Tucker, Jr., and K. H. Johnson, Chem. Phys. Lett. 36, 423 (1975).
- 31. L. L. Kesmodel, private communication.
- 32. R. B. King, *Transition-Metal Organometallic Chemistry*, Academic Press, Inc., New York, 1969, p. 25.
- 33. See for example L. D. Pettit and D. S. Barnes, *Fortschr. der Chemie* 28, 85 (1975), p. 121.
- 34. D. F. Dance and I. C. Walker, J. Chem. Soc. Faraday Trans. II 70, 1426 (1974).
- 35. E. H. Van Veen, Chem. Phys. Lett. 41, 540 (1976).
- R. J. Smith, J. Anderson, and G. J. Lapeyre, *Phys. Rev. Lett.* 37, 1081 (1976).
- G. Apai, P. S. Wehner, R. S. Williams, J. Stohr, and D. A. Shirley, *Phys. Rev. Lett.* 37, 1497 (1976).

Received March 22, 1977; revised October 6, 1977

The author is located at the IBM Thomas J. Watson Research Center, Yorktown Heights, New York 10598.